

Article

# Nonadiabatic Atomic-like State Stabilizing Antiferromagnetism and Mott Insulation in MnO

Ekkehard Krüger 

Institut für Materialwissenschaft, Materialphysik, Universität Stuttgart, D-70569 Stuttgart, Germany

Received: date; Accepted: date; Published: date

**Abstract:** In this paper I report evidence that the antiferromagnetic and insulating ground state of MnO is caused by a nonadiabatic atomic-like motion as it is evidently the case in NiO. In addition, I show that the experimental findings of Goodwin et al. [Phys. Rev. Lett. (2006), 96, 047209] corroborate my suggestion that the rhombohedral-like distortion in antiferromagnetic MnO as well as in antiferromagnetic NiO is an inner distortion of the monoclinic base-centered Bravais lattice of the antiferromagnetic phases.

**Keywords:** MnO; antiferromagnetic eigenstate; Mott insulator; atomic-like motion; nonadiabatic Heisenberg model; magnetic band; magnetic super band; group theory

## 1. Introduction

Manganese monoxide is antiferromagnetic with the Néel temperature  $T_N = 122\text{K}$  [1,2]. Above  $T_N$ , MnO possesses the fcc structure  $Fm3m = \Gamma_c^f O_h^5$  (225) (in parentheses I always give the international number). Just as in antiferromagnetic NiO, the magnetic structure of antiferromagnetic MnO is invariant under the monoclinic base-centered magnetic group  $C_c2/c$  [3] which will be given explicitly in Eq. (1). The antiferromagnetic state is accompanied by a small rhombohedral-like contraction of the crystal along one of the triad axes [4], which evidently forms an inner deformation of the monoclinic base-centered Bravais lattice  $\Gamma_m^b$  [5]. The physical origin of the rhombohedral-like contraction in MnO is clearly the same as in NiO since the concerned magnetic groups are the same. So, I give in Sections 2 and 3 only a brief summary of Sections 3 and 4 of [5] to make the paper selfcontained. These sections provide the magnetic group of the antiferromagnetic state and repeat the definition of the term “rhombohedral-like contraction” used in the following sections.

In Section 4 the experimental findings of Goodwin et al. [4] will be interpreted. They corroborate my concept of the rhombohedral-like contraction being an *inner* deformation of the monoclinic base-centered Bravais lattice of antiferromagnetic MnO (and NiO).

Also the other electronic features of MnO are very similar to those of NiO: both are antiferromagnetic under the respective Néel temperatures, and both are Mott insulators in the antiferromagnetic as well as in the paramagnetic phase [6]. Hence, the stability of the antiferromagnetic and the insulating state of MnO should be caused by a nonadiabatic atomic-like motion as it is evidently the case in NiO. In this paper I report evidence that this is true, i.e., that a suited nonadiabatic atomic-like motion exists also in MnO. The starting points are the conventional band structures of paramagnetic and antiferromagnetic MnO. In Section 5 I will explain the characteristics of the conventional band structures as used in this paper. On the basis of the symmetry of the Bloch functions in the band structure of MnO, I apply in Section 6 the group-theoretical nonadiabatic Heisenberg model (NHM) [7] to paramagnetic and antiferromagnetic MnO. First, in Section 6.1 I will show that there exists best localized symmetry-adapted Wannier functions at the Fermi level of paramagnetic MnO qualifying this material to be a Mott insulator. In the following Section 6.2 I will show that the nonadiabatic atomic-like motion of the electrons in antiferromagnetic

MnO stabilizes not only the antiferromagnetic state but provides also an ideal precondition for the Mott condition to be effective in antiferromagnetic MnO.

## 2. Magnetic group of the antiferromagnetic state

This section is a brief summary of Section 3 of [5] providing the terms needed in Sections 4 and 6. The antiferromagnetic structure of MnO is invariant under the symmetry operations of the type IV Shubnikov magnetic group  $C_c2/c$  [3] which may be written as [8]

$$C_c2/c = C2/c + K\{E|\tau\}C2/c, \quad (1)$$

where  $K$  denotes the anti-unitary operator of time-inversion,  $E$  stands for the identity operation, and

$$\tau = \frac{1}{2}T_1 \quad (2)$$

is the non-primitive translation in the group  $C2/c$  as indicated in Figure 1.

The unitary subgroup  $C2/c$  (15) of  $C_c2/c$  is based on the monoclinic base-centered Bravais lattice  $\Gamma_m^b$  and contains (besides the pure translations) the 4 elements given in Equation (2) of [5]. As in [5], I refer the magnetic group  $C_c2/c$  to as  $M_{15}$  because its unitary subgroup  $C2/c$  bears the international number 15,

$$M_{15} = C2/c + K\{E|\tau\}C2/c. \quad (3)$$

Though the magnetic group  $M_{15}$  leaves invariant the antiferromagnetic structure of MnO, it is not the magnetic group of antiferromagnetic MnO because it does not possess suitable co-representations. Instead it is the subgroup

$$M_9 = Cc + K\{C_{2b}|\mathbf{0}\}Cc \quad (4)$$

of  $M_{15}$  allowing the system to have eigenstates with the experimentally observed antiferromagnetic structure [5]. The symmetry operation  $C_{2b}$  is the rotation through  $\pi$  as indicated in Figure 1. Just as  $M_{15}$ ,  $M_9$  is based on the monoclinic base-centered Bravais lattice  $\Gamma_m^b$ . The unitary subgroup  $Cc$  (9) of  $M_9$  contains (besides the pure translations) two elements,

$$Cc = \left\{ \{E|\mathbf{0}\}, \{\sigma_{db}|\tau\} \right\}, \quad (5)$$

where  $\sigma_{db}$  stands for the reflection  $\sigma_{db} = IC_{2b}$  and  $I$  denotes the inversion.

Magnetoscriction alone produces the magnetic group  $M_{15}$  in MnO. Consequently, in addition to the magnetoscriction, the crystal must be distorted in such a way that the Hamiltonian of the nonadiabatic electron system still commutes with the elements of  $M_9$ , but does not commute with the symmetry operations of  $M_{15} - M_9$ . This is achieved by exactly the one distortion of the crystal illustrated in Figure 1: The Mn atoms are shifted in  $\pm(T_2 - T_3)$  direction from their positions at the lattice points  $t_{Mn}$  in Eq. (6), realizing in this way the group  $M_9$  [5].

## 3. Rhombohedral-like distortion

As well as antiferromagnetic NiO, antiferromagnetic MnO is slightly deformed by a rhombohedral-like distortion which may be interpreted as inner distortion of the base-centered monoclinic Bravais lattice  $\Gamma_m^b$  [5]. With “inner distortion” I want to emphasize that the rhombohedral-like distortion does not break the symmetry of the magnetic group  $M_9$ . Figure 1 shows the dislocations of the Mn

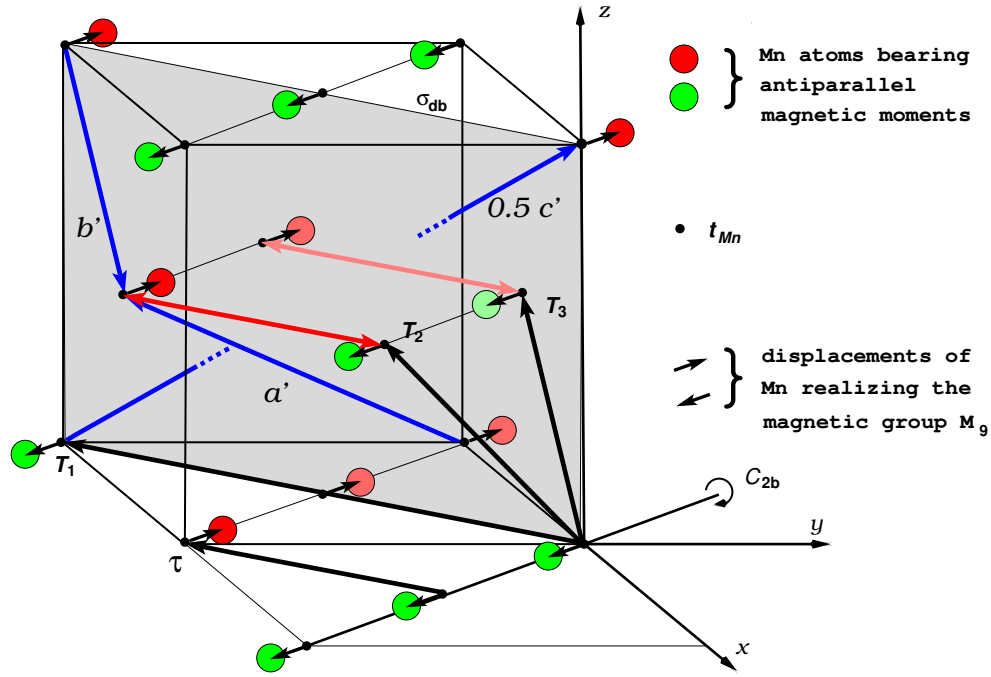


**Figure 1.** Mangan atoms in distorted antiferromagnetic MnO possessing the magnetic group  $M_9$  (Eq. (4)) based on the monoclinic base-centered Bravais lattice  $\Gamma_m^b$ . The Mn atoms represented by red circles bear a magnetic moment parallel or antiparallel to  $[11\bar{2}]$  and the atoms represented by green circles the opposite moment. The vectors  $T_i$  are the basic translations of  $\Gamma_m^b$ .

atoms stabilizing, on the one hand, the antiferromagnetic structure and producing, on the other hand, the rhombohedral-like distortion, as is substantiated in [5].

For the sake of clarity, the basic vectors of the Bravais lattice  $\Gamma_m^b$  of  $M_9$  are embedded in the paramagnetic fcc lattice of MnO. Therefore, this Figure is also somewhat misleading because the fcc lattice no longer exists in the antiferromagnetic phase. It is distorted as a whole whereby the vectors  $T_1$ ,  $T_2$ , and  $T_3$  stay basic vectors of  $\Gamma_m^b$ . The lattice points  $t_{Mn}$  plotted in Figure 1 are not the positions of Mn in the fcc lattice, but are defined by the equations:

$$\begin{aligned} t_{Mn} &= n_1 T_1 + n_2 T_2 + n_3 T_3 \quad \text{or} \\ t_{Mn} &= \frac{1}{2} T_1 + n_1 T_1 + n_2 T_2 + n_3 T_3, \end{aligned} \quad (6)$$

where  $T_1$ ,  $T_2$ , and  $T_3$  are the basic vectors of  $\Gamma_m^b$  and  $n_1$ ,  $n_2$ , and  $n_3$  are integers. Thus, the vectors  $t_{Mn}$  are solely given in terms of the basic vectors of  $\Gamma_m^b$  detached from the paramagnetic fcc lattice.

#### 4. Interpretation of the experimental findings of Goodwin et al.

Goodwin et al. [4] determined the displacements of the Mn and O atoms in the true monoclinic structure from their positions in an assumed rhombohedral structure and gave the result in Table I of their

paper. They use the coordinates  $\mathbf{a}'$ ,  $\mathbf{b}'$  and  $\mathbf{c}'$  depicted in Figure 1 by the blue vectors, depending on the translations of the base-centered monoclinic Bravais lattice according to

$$\begin{aligned} \mathbf{a}' &= 2\mathbf{T}_2 - \mathbf{T}_3 \\ \mathbf{b}' &= -\mathbf{T}_3 \\ \mathbf{c}' &= -3\mathbf{T}_1 + 2\mathbf{T}_2 + 2\mathbf{T}_3, \end{aligned} \quad (7)$$

see Figure 1. From Table I of Ref. [4] we get for the displacement  $\Delta$  of a Mn1 atom

$$\Delta = \alpha \mathbf{a}' + \beta \mathbf{b}' + \gamma \mathbf{c}' \quad (8)$$

which may be written as

$$\Delta = -3\gamma \mathbf{T}_1 + \frac{3\alpha + \beta}{2}(\mathbf{T}_2 - \mathbf{T}_3) + \frac{\alpha - \beta + 4\gamma}{2}(\mathbf{T}_2 + \mathbf{T}_3), \quad (9)$$

leading with  $\alpha = -2.072 \cdot 10^{-3}$ ,  $\beta = 10.11 \cdot 10^{-3}$ , and  $\gamma = 2.708 \cdot 10^{-3}$  (Table I of [4]) to

$$\Delta = -8.124\mathbf{T}_1 + 1.947(\mathbf{T}_2 - \mathbf{T}_3) - 0.675(\mathbf{T}_2 + \mathbf{T}_3), \quad (10)$$

omitting the common factor  $10^{-3}$ .

The vectors  $\mathbf{T}_1$  and  $(\mathbf{T}_2 + \mathbf{T}_3)$  lie in the plane related to the reflection  $\sigma_{db}$ , shortly referred to as “the plane  $\sigma_{db}$ ” as depicted in Figure 1. Hence, the first and the third summand in (10) describe a displacement of the Mn atoms parallel to the plane  $\sigma_{db}$  resulting from a modification of the translations  $\mathbf{T}_1$ ,  $\mathbf{T}_2$ , and  $\mathbf{T}_3$  occurring in such a way that the  $\mathbf{T}_i$  stay basis vectors of the base-centered monoclinic Bravais lattice [5]. Consequently, these summands are caused by a deformation of the crystal as a whole being still invariant under the translations of the monoclinic lattice.

The second summand, on the other hand, describes a shift of the Mn atoms perpendicular the the plane  $\sigma_{db}$ . It cannot be the result of a modification of the lattice vectors  $\mathbf{T}_i$  because such a modification would destroy the base-centered monoclinic Bravais lattice. These shifts of the Mn atoms in  $\pm(\mathbf{T}_2 - \mathbf{T}_3)$  directions clearly identify the base-centered monoclinic magnetic group  $M_9$  as the magnetic group of antiferromagnetic MnO because  $M_9$  is the only magnetic group invariant under both the antiferromagnetic structure and a shift of the Mn atoms perpendicular to the plane  $\sigma_{db}$  [5]. Thus, we may interpret this result of Goodwin et al. as follows:

- (i) The significant shifts of the Mn atoms in  $\pm(\mathbf{T}_2 - \mathbf{T}_3)$  direction realize the magnetic group  $M_9$  and stabilize in this way the antiferromagnetic structure, see Section 2.
- (ii) The observed displacements of the Mn atoms in Equation (10) are greatest in  $\mathbf{T}_1$  direction, they are even 12 times greater than in  $(\mathbf{T}_2 + \mathbf{T}_3)$  direction. This corroborates my supposition [5] that the mutual attraction between Mn atoms with opposite shifts in  $\pm(\mathbf{T}_2 - \mathbf{T}_3)$  direction is mainly responsible for the rhombohedral-like deformation of the crystal. The displacements are maximal in  $\mathbf{T}_1$  direction since in this direction they are parallel to the plane  $\sigma_{db}$  and, thus, do not destroy the magnetic group  $M_9$ , as is illustrated by the red line in Figure 1.

Furthermore, Goodwin et al. found that the symmetry of the threefold rotational axis implicit in a rhombohedral lattice is (slightly) broken in MnO. This demonstrates again that we only have a rhombohedral-like deformation rather than an (exact) rhombohedral symmetry in antiferromagnetic MnO (just as in antiferromagnetic NiO [5]). On the other hand, a break of the monoclinic base-centered

symmetry with the magnetic group  $M_9$  must not happen because this would destabilize the magnetic structure of MnO.

The small dislocations of the O atoms in  $c'$  direction (i.e., parallel to  $\sigma_{db}$ ) observed by Goodwin et al. are simply the result of the modification of the translations  $T_1$ ,  $T_2$ , and  $T_3$  produced by the Mn atoms. The O atoms do not actively deform the crystal.

## 5. Conventional band structure

The conventional band structure of paramagnetic MnO in Figure 2 is calculated by the FHI-aims (“Fritz Haber Institute ab initio molecular simulations”) computer program using the density functional theory (DFT) [9,10] to compute the total energy  $E_k$  of the Bloch states in the Brillouin zone. By “conventional band structure”, I mean a pure one-electron band-structure not taking into account any correlation effects. The strong correlation effects responsible for the stable antiferromagnetic state and the nonmetallic behavior of MnO enter by the postulates [7] of the group-theoretical NHM defining a strongly correlated nonadiabatic atomic-like motion at the Fermi level.

The NHM uses only a more qualitative run of the energy  $E_k$  in the band structure. It is the symmetry of the Bloch states in the points of symmetry of the Brillouin zone which characterizes an energy band within the NHM. The FHI-aims program uses spherical harmonics as basis functions and provides the possibility of an output of the special linear combinations of these functions used at a point  $k$ . Thus, I was able to write a C++ program to determine the symmetry of the Bloch functions at the points of symmetry in the Brillouin zone using the symmetry of the spherical harmonics as given in [8].

## 6. Symmetry-adapted and optimally localized Wannier functions in MnO

The NHM defines in narrow, partly filled electronic energy bands a strongly correlated nonadiabatic atomic-like motion stabilized by the nonadiabatic condensation energy  $\Delta E$  defined in Equation (2.20) of [7]. This atomic-like motion is not represented by atomic or hybrid atomic functions, but strictly by symmetry-adapted and optimally localized Wannier functions forming an (exact) unitary transformation of the Bloch functions of the energy band under consideration [7,11]. When the band is roughly half-filled and one of narrowest bands in the band structure, the special symmetry and spin-dependence of these Wannier functions qualifies a material to be superconducting [11–13], magnetic [11,14–16], or a Mott insulator [5,16]. In the following Subsection 6.1 I will show that paramagnetic MnO possesses optimally localized Wannier functions including all the electrons at the Fermi level and adapted to the fcc symmetry of the paramagnetic phase. These functions define a nonadiabatic atomic-like motion evidently responsible for the Mott insulation. In the second Subsection 6.2 I will show that the electrons near the Fermi level of antiferromagnetic MnO can be represented by Wannier functions comprising all the electrons at the Fermi level and adapted to the magnetic group  $M_9$  of the antiferromagnetic phase. The nonadiabatic atomic-like motion represented by these Wannier functions evidently stabilizes both the antiferromagnetic state and the Mott insulation.

### 6.1. Wannier functions symmetry-adapted to the paramagnetic fcc structure

All the information we need in this section is given in Figure 2 and Table 1. Figure 2 shows the conventional band structure of paramagnetic MnO and Table 1 is an excerpt of Table 1 of [17]. While Table 1 of [17] lists *all* the optimally localized symmetry-adapted Wannier functions in MnO centered at the Mn or O atoms and adapted to the paramagnetic space group  $Fm3m$  (225), Table 1 lists only the two bands with Wannier functions of  $\Gamma_3^+$  and  $\Gamma_5^+$  symmetry centered at the Mn atoms. The bands have two and three branches, respectively, yielding together five Wannier functions at each Mn atom.

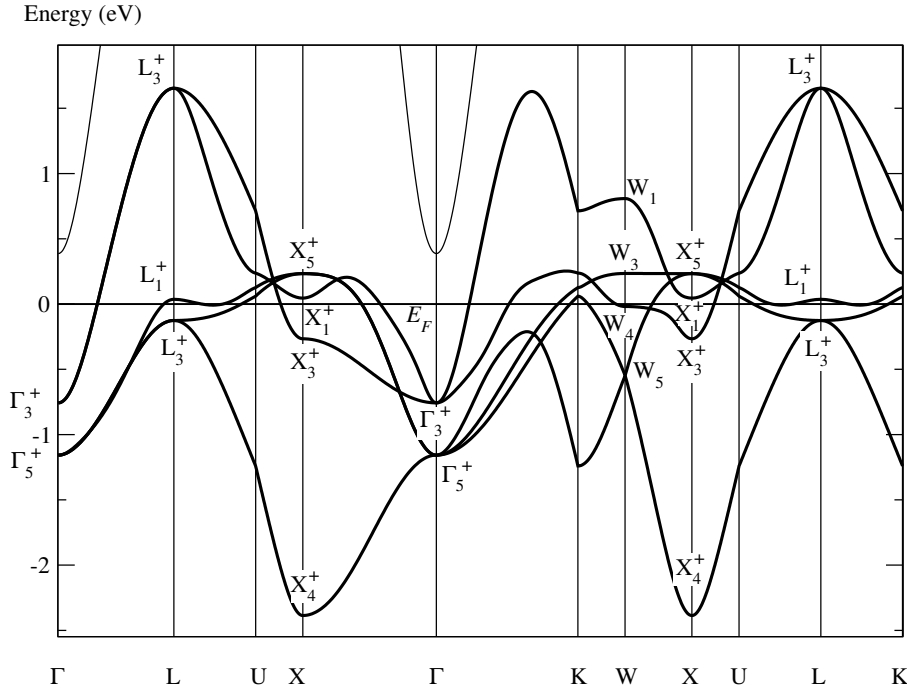


**Figure 2.** Conventional (Section 5) band structure of paramagnetic fcc MnO as calculated by the FHI-aims program [9,10], using the length  $a = 4.426\text{\AA}$  of the fcc paramagnetic unit cell given in Ref. [1], with symmetry labels determined by the author. The notations of the points of symmetry in the Brillouin zone for  $\Gamma_c^f$  follow Figure 3.14 of Ref. [8] and the symmetry labels are defined in Table A1 of [5]. The band highlighted by the bold lines forms an insulating band of  $d$  symmetry consisting of 5 branches.

By inspection of Figure 2 and Table 1 we recognize that the closed band highlighted by the bold lines in the band structure of paramagnetic MnO is characterized by the symmetry

$$\Gamma_3^+ + \Gamma_5^+, L_3^+ + L_1^+ + L_3^-, X_5^+ + X_1^+ + X_3^+ + X_4^+, W_1 + W_3 + W_4 + W_5 \quad (11)$$

of the two bands in Table 1 with Wannier functions centered at the Mn atoms. The set of these five Wannier functions has  $d$  symmetry since an atomic  $d$  orbital splits into a  $\Gamma_3^+$  and a  $\Gamma_5^+$  state in the fcc crystal field, see Table 2.7 of [8]. On the other hand, no partly filled band in the band structure of paramagnetic MnO possesses the symmetry of any band in Table 1 b of [17], listing the bands with Wannier functions centered at the O atoms. Hence, the energy band (11) originates entirely from a  $d$  orbital of Mn. This  $d$  band is an insulating band qualifying paramagnetic MnO to be a Mott insulator because it consists of all the branches crossing the Fermi level [17].

## 6.2. Wannier functions symmetry-adapted to the antiferromagnetic structure

All the information we now need is given in Figure 3 and in Table 2. This table is a shortened copy of Table A2 of [5] omitting the detailed notes to this Table in [5] (of course, these notes are also valid for Table 2 in this paper when “Ni” is replaced by “Mn”). Table 2 lists all the optimally localized Wannier

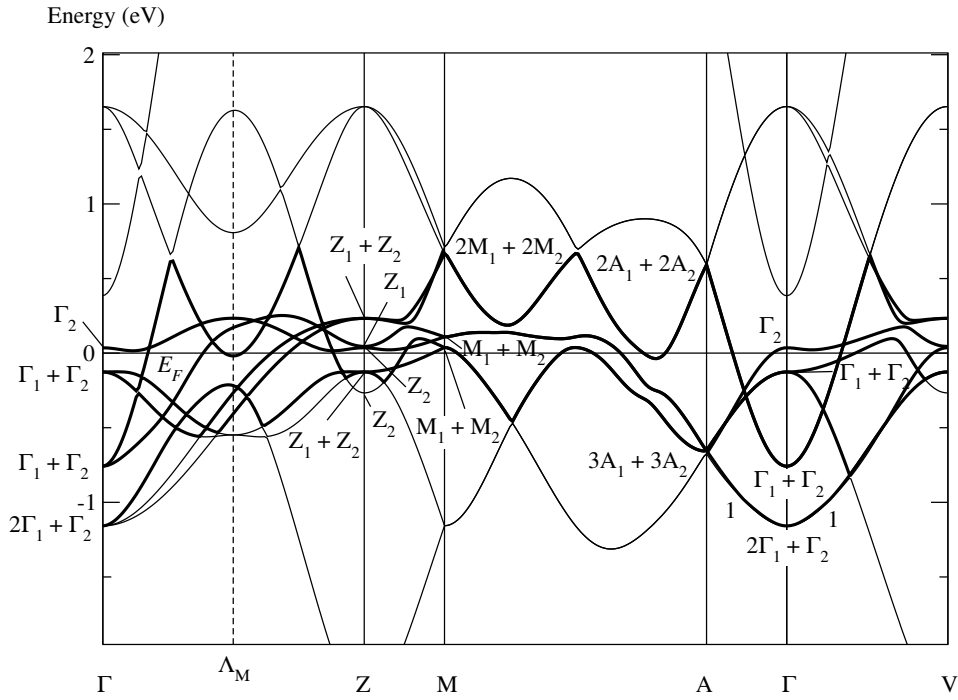


**Figure 3.** The band structure of MnO given in Figure 2 folded into the Brillouin zone for the monoclinic base centered Bravais lattice  $\Gamma_m^b$  of the magnetic group  $M_9$ . The band highlighted by the bold lines forms a magnetic super band consisting of six branches assigned to the manganese or oxygen atoms. The symmetry labels are defined in Table A4 of [5] and are determined from Figure 2 by means of Table A5 of [5]. The notations of the points of symmetry follow Figure 3.4 of Ref. [8]. The midpoint  $\Lambda_M$  of the line  $\bar{\Gamma}\bar{Z}$  is equivalent to the points  $W'(\frac{1}{4}\frac{1}{4}\frac{1}{2})$  and  $\Sigma'(\frac{1}{4}\frac{1}{4}0)$  in the Brillouin zone for the paramagnetic fcc lattice. The number “1” on the line  $\bar{A}\bar{\Gamma}\bar{V}$  indicates that here only one branch belongs to the magnetic band.

**Table 1.** Symmetry labels of the Bloch functions at the points of symmetry in the Brillouin zone for  $Fm\bar{3}m$  (225) of two energy bands with symmetry-adapted and optimally localized Wannier functions centered at the Mn atoms

	Mn(000)	$\Gamma$	X	L	W
Band 5	$\Gamma_3^+$	$\Gamma_3^+$	$X_1^+ + X_3^+$	$L_3^+$	$W_1 + W_4$
Band 8	$\Gamma_5^+$	$\Gamma_5^+$	$X_4^+ + X_5^+$	$L_1^+ + L_3^+$	$W_3 + W_5$

#### Notes to Table 1

- (i) The notations of the points of symmetry in the Brillouin zone for  $\Gamma_c^f$  follow Figure 3.14 of Ref. [8], and the symmetry notations of the Bloch functions are defined in Table A1 of [5].
- (ii) The bands are determined following Theorem 5 of [11], cf. Section 2 of [17].
- (iii) The point group  $G_{0Mn}$  of the positions [11] of the Mn atoms are equal to the full cubic point group  $O_h$ . The Wannier functions belong to the representation of  $G_{0Mn}$  included below the atom.

functions centered at the Mn or O atoms and symmetry-adapted to the magnetic group  $M_9$ . In both cases, there exists only one band with coinciding symmetries.

When folding the band structure of paramagnetic MnO given in Figure 2 into the Brillouin zone of the monoclinic-base centered magnetic structure, we receive the band structure plotted in Figure 3. The narrow band highlighted by the bold lines comprises six branches with the symmetry

$$3\Gamma_1 + 3\Gamma_2, 3Z_1 + 3Z_2, 3M_1 + 3M_2, 3A_1 + 3A_2. \quad (15)$$

Thus, band 1 (with two branches) listed in Table 2 (a) as well as band 1 in Table 2 (b) exists three times in the band structure of antiferromagnetic MnO. Hence, we may unitarily transform the Bloch functions of this band into optimally localized Wannier functions symmetry adapted to the magnetic group  $M_9$ . In doing so, we first have four possibilities: we may generate either six Wannier functions centered at the two Manganese atoms (with three Wannier functions at  $Mn_1$  and three Wannier functions at  $Mn_2$ ), four Wannier functions centered at the manganese atoms and two Wannier functions centered at the oxygen atoms, two Wannier functions centered at the manganese atoms and four Wannier functions centered at the oxygen atoms, or six Wannier functions centered at the oxygen atoms in the unit cell. The first possibility does certainly not lead to a stable atomic-like state as consequence of the Coulomb repulsion between localized states at the same position, and the last possibility has no physical significance because it does not provide localized states at the Mn atoms which bear the magnetic moments. In the remaining two cases the highlighted band is a magnetic band. It provides localized Wannier states allowing the electrons to perform a nonadiabatic atomic-like motion stabilizing a magnetic state with the magnetic group  $M_9$  [5,14]. Moreover, it is a magnetic super band since it comprises all the branches crossing the Fermi level and, consequently, qualifying MnO to be a Mott insulator also in the antiferromagnetic phase [5].

## 7. Results

The paper is concerned with three striking features of MnO:

- (i) The insulating ground state of both paramagnetic and antiferromagnetic MnO,
- (ii) the stability of the antiferromagnetic state,
- (iii) the rhombohedral-like deformation in the antiferromagnetic phase,



**Table 2.** Symmetry labels of the Bloch functions at the points of symmetry in the Brillouin zone for  $Cc$  (9) of all the energy bands with symmetry-adapted and optimally localized Wannier functions centered at the Mn (Table (a)) and O (Table (b)) atoms, respectively.

(a) <b>Mn</b>	$Mn_1(000)$	$Mn_2(\frac{1}{2}00)$	$K\{C_{2b} \mathbf{0}\}$	$\Gamma$	$A$	$Z$	$M$	$L$	$V$
Band 1	$d_1$	$d_1$	OK	$\Gamma_1 + \Gamma_2$	$A_1 + A_2$	$Z_1 + Z_2$	$M_1 + M_2$	$2L_1$	$2V_1$

(b) <b>O</b>	$O_1(\frac{1}{4}\frac{1}{2}\frac{1}{2})$	$O_2(\frac{3}{4}\frac{1}{2}\frac{1}{2})$	$K\{C_{2b} \mathbf{0}\}$	$\Gamma$	$A$	$Z$	$M$	$L$	$V$
Band 1	$d_1$	$d_1$	OK	$\Gamma_1 + \Gamma_2$	$A_1 + A_2$	$Z_1 + Z_2$	$M_1 + M_2$	$2L_1$	$2V_1$

#### Notes to Table 2

- (i) The notations of the points of symmetry in the Brillouin zone for  $\Gamma_m^b$  follow Figure 3.4 of Ref. [8] and the symmetry notations of the Bloch functions are defined in Table A4 of [5].
- (ii) The bands are determined following Theorem 5 of [11].
- (iii) The point groups  $G_{0Mn}$  and  $G_{0O}$  of the positions [11] of the Mn respective O atoms contain, in each case, only the identity operation:

$$G_{0Mn} = G_{0O} = \{ \{E|\mathbf{0}\} \}. \quad (12)$$

Thus, the Wannier functions at the Mn or O atoms belong to the simple representation

$$\frac{\{E|\mathbf{0}\}}{d_1 \quad 1}$$

of  $G_{0Mn}$  and  $G_{0O}$ .

- (iv) The symmetry of band 1 in Table 2 (a) coincides fully with the symmetry of band 1 in Table 2 (b).
- (v) Each row defines a band consisting of two branches with Bloch functions that can be unitarily transformed into Wannier functions being:
  - as well localized as possible;
  - centered at the  $Mn_1$  and  $Mn_2$  (Table (a)) or  $O_1$  and  $O_2$  (Table (b)) atoms; and
  - symmetry adapted to the unitary subgroup  $Cc$  (9) of the magnetic group  $M_9$  according to

$$\begin{aligned} P(\{\sigma_{db}|\boldsymbol{\tau}\})w_{Mn_1}(\mathbf{r}) &= w_{Mn_2}(\mathbf{r}), \\ P(\{\sigma_{db}|\boldsymbol{\tau}\})w_{Mn_2}(\mathbf{r}) &= w_{Mn_1}(\mathbf{r}), \\ P(\{\sigma_{db}|\boldsymbol{\tau}\})w_{O_1}(\mathbf{r}) &= w_{O_2}(\mathbf{r}), \\ P(\{\sigma_{db}|\boldsymbol{\tau}\})w_{O_2}(\mathbf{r}) &= w_{O_1}(\mathbf{r}); \end{aligned} \quad (13)$$

where  $w_{Mn_1}(\mathbf{r})$ ,  $w_{Mn_2}(\mathbf{r})$ ,  $w_{O_1}(\mathbf{r})$ , and  $w_{O_2}(\mathbf{r})$  denote the Wannier functions centered at the Mn and O atoms, respectively.

- The entry “OK” indicates that the Wannier functions follow also Theorem 7 of Ref. [11] and, consequently, may be chosen symmetry-adapted to the magnetic group  $M_9$ . Thus, in addition to Equation (13), we have:

$$\begin{aligned} KP(\{C_{2b}|\mathbf{0}\})w_{Mn_1}(\mathbf{r}) &= w_{Mn_1}(\mathbf{r}), \\ KP(\{C_{2b}|\mathbf{0}\})w_{Mn_2}(\mathbf{r}) &= w_{Mn_2}(\mathbf{r}), \\ KP(\{C_{2b}|\mathbf{0}\})w_{O_1}(\mathbf{r}) &= w_{O_2}(\mathbf{r}), \\ KP(\{C_{2b}|\mathbf{0}\})w_{O_2}(\mathbf{r}) &= w_{O_1}(\mathbf{r}), \end{aligned} \quad (14)$$

cf. the more detailed notes to Table A2 in [5].

characterizing likewise the isomorphic transition-metal monoxide NiO. The aim of this paper was to show that these striking electronic properties of MnO have the same physical origin as in NiO: Just as in NiO [5],

- the antiferromagnetic state in MnO is evidently stabilized by the nonadiabatic atomic-like motion in a magnetic band. This magnetic band is even a magnetic super band because it comprises all the electrons at the Fermi level. Thus, the special atomic-like motion in this band qualifies antiferromagnetic MnO to be a Mott insulator.
- the Bloch functions of a (roughly) half-filled energy band in the paramagnetic band structure of MnO can be unitarily transformed into optimally localized Wannier functions symmetry-adapted to the fcc symmetry of the paramagnetic phase. These Wannier functions are situated at the Mn atoms, have  $d$  symmetry and comprise all the electrons at the Fermi level. Thus, the atomic-like motion represented by these Wannier functions qualifies also paramagnetic MnO to be a Mott insulator.
- the magnetic structure is stabilized by a shift of the Mn atoms in  $\pm(T_2 - T_3)$  direction. These shifts evidently produce the rhombohedral-like deformation of the crystal because the attraction between the Mn atoms increases slightly when the Mn atoms are shifted in opposite directions. This concept presented in [5] is corroborated by the experimental observations of Goodwin et al. [4].
- the rhombohedral-like distortion does not possess a rhombohedral (trigonal) space group but is an inner distortion of the base-centered monoclinic magnetic group  $M_9$  in Equation (4). The group  $M_9$ , on the other hand, must not be broken because it stabilizes the antiferromagnetic structure.

## 8. Discussion

The results of this paper demonstrate once more that the nonadiabatic atomic-like motion defined within the NHM has physical reality. So they confirm my former findings suggesting that superconductivity [11–13], magnetism [11,14–16] and Mott insulation [5,16,17] are produced by the nonadiabatic atomic-like motion defined within the NHM.

In addition, the paper corroborates my former suggestion [5,14,18] that we can determine by group theory whether or not a magnetic state with the magnetic group  $M$  may be an eigenstate in a system invariant under time inversion.

**Funding:** This publication was supported by the Open Access Publishing Fund of the University of Stuttgart.

**Acknowledgments:** I am very indebted to Guido Schmitz for his support of my work.

**Conflicts of Interest:** The author declares no conflict of interest.

## Abbreviations

The following abbreviations are used in this manuscript:

NHM	Nonadiabatic Heisenberg model
$E$	Identity operation
$I$	Inversion
$C_{2b}$	Rotation through $\pi$ as indicated in Figure 1
$\sigma_{db}$	Reflection $IC_{2b}$
$K$	anti-unitary operator of time inversion

## References

1. Shull, C.G.; Strauser, W.A.; Wollan, E.O. Neutron Diffraction by Paramagnetic and Antiferromagnetic Substances. *Phys. Rev.* **1951**, *83*, 333–345. doi:10.1103/PhysRev.83.333.
2. Roth, W.L. Magnetic Structures of MnO, FeO, CoO, and NiO. *Phys. Rev.* **1958**, *110*, 1333–1341. doi:10.1103/PhysRev.110.1333.

3. Cracknell, A.P.; Joshua, S.J. The space group corepresentations of antiferromagnetic NiO. *Mathematical Proceedings of the Cambridge Philosophical Society* **1969**, *66*, 493–504. doi:10.1017/S0305004100045229.
4. Goodwin, A.L.; Tucker, M.G.; Dove, M.T.; Keen, D.A. Magnetic Structure of MnO at 10 K from Total Neutron Scattering Data. *Phys. Rev. Lett.* **2006**, *96*, 047209. doi:10.1103/PhysRevLett.96.047209.
5. Krüger, E. Structural Distortion Stabilizing the Antiferromagnetic and Insulating Ground State of NiO. *Symmetry* **2019**, *12*. doi:10.3390/sym12010056.
6. Austin, I.G.; Mott, N.F. Metallic and Nonmetallic Behavior in Transition Metal Oxides. *Science* **1970**, *168*, 71–77. doi:10.1126/science.168.3927.71.
7. Krüger, E. Nonadiabatic extension of the Heisenberg model. *Phys. Rev. B* **2001**, *63*, 144403–1–13. doi:10.1103/PhysRevB.63.144403.
8. Bradley, C.; A.P. Cracknell. *The Mathematical Theory of Symmetry in Solids*; Clarendon, Oxford, 1972.
9. Blum, V.; Gehrke, R.; Hanke, F.; Havu, P.; Havu, V.; Ren, X.; Reuter, K.; Scheffler, M. Ab initio molecular simulations with numeric atom-centered orbitals. *Computer Physics Communications* **2009**, *180*, 2175 – 2196.
10. Havu, V.; Blum, V.; Havu, P.; Scheffler, M. Efficient O(N)<sup>2</sup> integration for all-electron electronic structure calculation using numeric basis functions. *Computer Physics Communications* **2009**, *228*, 8367 – 8379.
11. Krüger, E.; Strunk, H.P. Group Theory of Wannier Functions Providing the Basis for a Deeper Understanding of Magnetism and Superconductivity. *Symmetry* **2015**, *7*, 561–598. doi:10.3390/sym7020561.
12. Krüger, E. Modified BCS Mechanism of Cooper Pair Formation in Narrow Energy Bands of Special Symmetry I. Band Structure of Niobium. *J. Supercond.* **2001**, *14*, 469–489. Please note that in this paper the term “superconducting band” was abbreviated by “ $\sigma$  band”, doi:10.1023/A:1012231428443.
13. Krüger, E. Constraining Forces Stabilizing Superconductivity in Bismuth. *Symmetry* **2018**, *10*. doi:10.3390/sym10020044.
14. Krüger, E. Stability and symmetry of the spin-density-wave-state in chromium. *Phys. Rev. B* **1989**, *40*, 11090–11103. doi:https://doi.org/10.1103/PhysRevB.40.11090.
15. Krüger, E. Energy band with Wannier functions of ferromagnetic symmetry as the cause of ferromagnetism in iron. *Phys. Rev. B* **1999**, *59*, 13795–13805. doi:https://doi.org/10.1103/PhysRevB.59.13795.
16. Krüger, E. Structural Distortion Stabilizing the Antiferromagnetic and Semiconducting Ground State of BaMn<sub>2</sub>As<sub>2</sub>. *Symmetry* **2016**, *8*(10), 99. doi:10.3390/sym8100099.
17. Krüger, E. Wannier States of FCC Symmetry Qualifying Paramagnetic NiO to Be a Mott Insulator. *Symmetry* **2020**, *12*. doi:10.3390/sym12050687.
18. Krüger, E.; Strunk, H.P. The Structural Distortion in Antiferromagnetic LaFeAsO Investigated by a Group-Theoretical Approach. *J. Supercond.* **2011**, *24*, 2103–2117. doi:10.1007/s10948-011-1177-6.